JGP Journal of General Physiology

ARTICLE

Alternative splicing potentiates dysfunction of early-onset epileptic encephalopathy *SCN2A* variants

Christopher H. Thompson[1a], Roy Ben-Shalom[2], Kevin J. Bender[2], and Alfred L. George Jr.[1]

Epileptic encephalopathies are severe forms of infantile-onset epilepsy often complicated by severe neurodevelopmental impairments. Some forms of early-onset epileptic encephalopathy (EOEE) have been associated with variants in *SCN2A*, which encodes the brain voltage-gated sodium channel $Na_V1.2$. Many voltage-gated sodium channel genes, including *SCN2A*, undergo developmentally regulated mRNA splicing. The early onset of these disorders suggests that developmentally regulated alternative splicing of $Na_V1.2$ may be an important consideration when elucidating the pathophysiological consequences of epilepsy-associated variants. We hypothesized that EOEE-associated $Na_V1.2$ variants would exhibit greater dysfunction in a splice isoform that is prominently expressed during early development. We engineered five EOEE-associated $Na_V1.2$ variants (T236S, E999K, S1336Y, T1623N, and R1882Q) into the adult and neonatal splice isoforms of $Na_V1.2$ and performed whole-cell voltage clamp to elucidate their functional properties. All variants exhibited functional defects that could enhance neuronal excitability. Three of the five variants (T236S, E999K, and S1336Y) exhibited greater dysfunction in the neonatal isoform compared with those observed in the adult isoform. Computational modeling of a developing cortical pyramidal neuron indicated that T236S, E999K, S1336Y, and R1882Q showed hyperexcitability preferentially in immature neurons. These results suggest that both splice isoform and neuronal developmental stage influence how EOEE-associated $Na_V1.2$ variants affect neuronal excitability.

Introduction

Variants in genes encoding voltage-gated sodium (Na_V) channels are associated with epilepsy and neurodevelopmental disorders with a wide range of severity (George, 2005; Oliva et al., 2012). This is illustrated by variants in *SCN2A* encoding the $Na_V1.2$ channel, which may be associated with relatively benign familial epilepsy (Heron et al., 2002; Berkovic et al., 2004; Herlenius et al., 2007; Misra et al., 2008), early-onset epileptic encephalopathy (EOEE; Beal et al., 2012; Nakamura et al., 2013; Touma et al., 2013; Howell et al., 2015; Wolff et al., 2017), autism spectrum disorder (O'Roak et al., 2011; Sanders et al., 2012; D'Gama et al., 2015; Ben-Shalom et al., 2017), or intellectual disability (Baasch et al., 2014; Sanders et al., 2018). One of the most severe conditions associated with *SCN2A* mutation is Ohtahara syndrome, which has onset within the first 2 wk of life and features intractable focal or generalized seizures sometimes accompanied by a suppression-burst pattern on electroencephalography (EEG), eventually manifesting with severe cognitive and neurodevelopmental impairment (Le Bouter et al., 2003; Nakamura et al., 2013; Touma et al., 2013; Zerem et al., 2014). The factors contributing to the very early onset and severity of Ohtahara syndrome and related disorders associated with $Na_V1.2$ variants are not entirely clear (Ogiwara et al., 2009).

Previous reports have suggested that the majority of EOEE-associated $Na_V1.2$ variants exert gain-of-function effects (Ben-Shalom et al., 2017; Berecki et al., 2018), although only a few variants have been studied. Because $Na_V1.2$ is strongly expressed in neocortical glutamatergic pyramidal neurons, where it localizes to axon initial segments (AISs), nodes of Ranvier, and the somatodendritic compartment in the developing brain, gain-of-function variants are predicted to enhance network excitability (Hu et al., 2009; Liao et al., 2010; Tian et al., 2014; Yamagata et al., 2017; Spratt et al., 2019). During maturation, $Na_V1.2$ is replaced at the distal AIS and nodes of Ranvier by $Na_V1.6$, suggesting that gain-of-function variants in $Na_V1.2$ may have less severe consequences on action potential initiation and propagation in mature neurons due to its diminished contribution to these processes (Hu et al., 2009; Liao et al., 2010; Tian et al., 2014). Consistent with this developmental switch in Na_V channel expression, recent work has suggested that sodium channel–blocking antiepileptic drugs are most effective in the setting of

[1]Department of Pharmacology, Northwestern University Feinberg School of Medicine, Chicago, IL; [2]Center for Integrative Neuroscience, Kavli Institute for Fundamental Neuroscience, Department of Neurology, University of California, San Francisco, San Francisco, CA.

Correspondence to Christopher H. Thompson: chris.thompson@northwestern.edu.

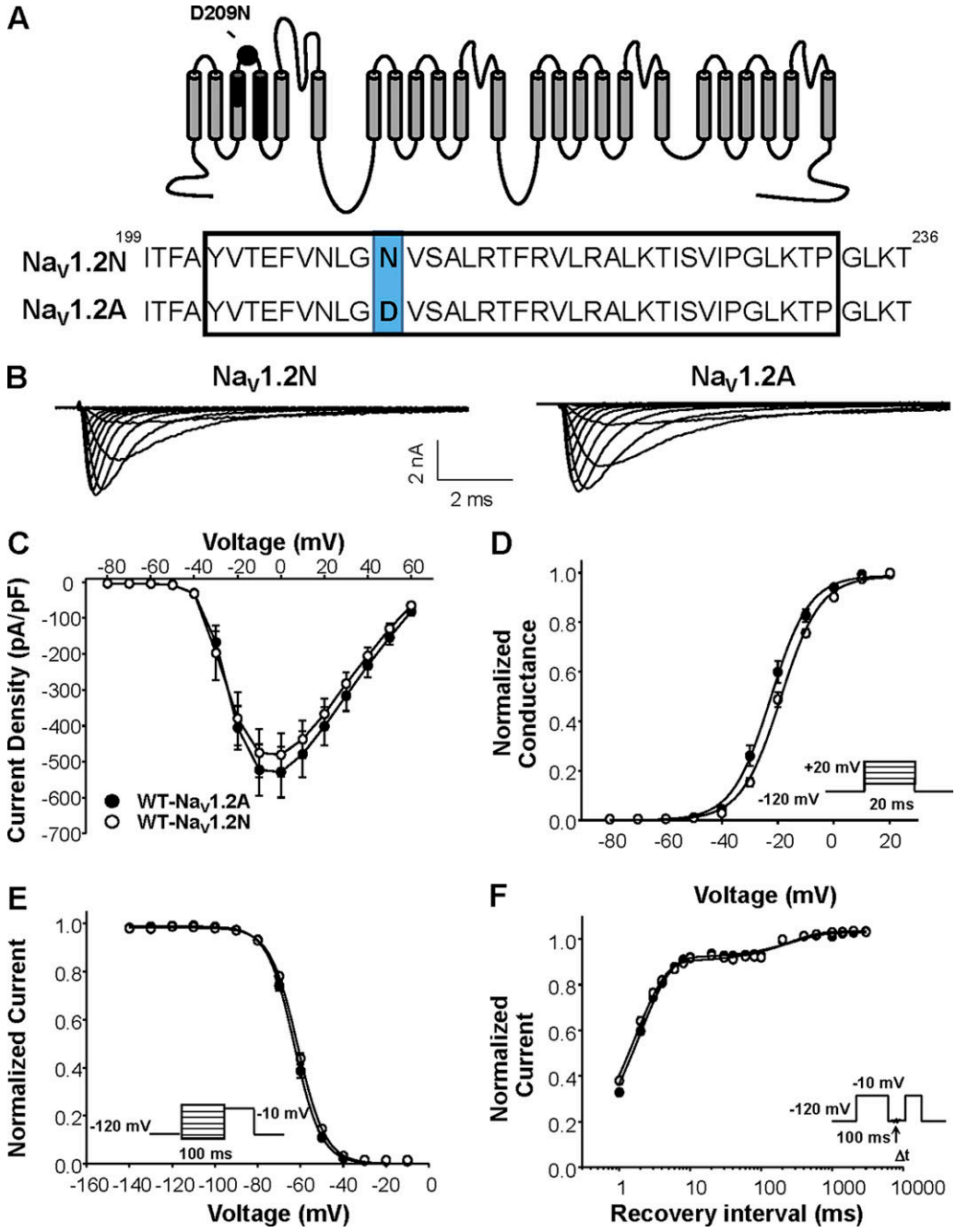

Figure 1. **Biophysical properties of $Na_V1.2$ splice variants. (A)** Top: Predicted transmembrane topology of $Na_V1.2$, highlighting the location of the exon 5 coding region (black shaded) and amino acid change associated with alternative exon splicing (black dot). Bottom: Amino acid alignment of $Na_V1.2N$ and $Na_V1.2A$. **(B)** Representative whole-cell sodium currents recorded from tsA201 cells coexpressing either $Na_V1.2N$ (left) or $Na_V1.2A$ (right) with β1 and β2 subunits. **(C)** Current density elicited by test pulses to various membrane potentials and normalized to cell capacitance. **(D)** Voltage dependence of channel activation. **(E)** Voltage dependence of channel inactivation. **(F)** Time-dependent recovery from inactivation. Closed symbols represent $Na_V1.2A$, and open symbols represent $Na_V1.2N$. All data are expressed as mean ± SEM for 15 measurements. Statistical comparisons were made using an unpaired Student's *t* test.

EOEE associated with gain-of-function $Na_V1.2$ variants (Wolff et al., 2017).

SCN2A undergoes developmentally regulated alternative mRNA splicing that leads to incorporation of an alternate exon encoding a portion of the domain I voltage-sensor (S3 and S4 helices). The two resulting protein isoforms (proteoforms) differ by one amino acid at position 209, encoding an asparagine in the splice proteoform expressed primarily during early development (neonatal proteoform, designated here as $Na_V1.2N$) and an aspartic acid in the proteoform expressed mainly in adult brain ($Na_V1.2A$). While this splicing event has been demonstrated in human brain tissue, the time course over which the transition from neonatal to adult proteoforms occurs is unknown (Kasai et al., 2001). In mouse cortex, the neonatal splice proteoform is

present in approximately twofold excess compared with the canonical adult-expressed $Na_V1.2A$ transcript in early development, but drops to one third of the canonical splice proteoform within the first 2 wk of life (Kasai et al., 2001; Copley, 2004; Gazina et al., 2010). An analogous splicing event affecting $Na_V1.1$ influences the pharmacological properties of that channel (Thompson et al., 2011). The contribution of alternative splicing to the pathogenesis of *SCN2A*-associated EOEE has not been systematically investigated, and prior studies determining the functional consequences of *SCN2A* variants were performed using the canonical splice proteoform expressed predominantly in adult brain (Misra et al., 2008; Ben-Shalom et al., 2017; Wolff et al., 2017; Berecki et al., 2018). However, some work suggests that variants in the neonatal splice proteoform negatively impact neuronal excitability (Xu et al., 2007; Gazina et al., 2015).

In this study, we examined the functional consequences of five $Na_V1.2$ variants (T236S, E999K, S1336Y, T1623N, and R1882Q) in both the neonatal and adult proteoforms. Four of the five variants were not previously studied for their functional effects, while R1882Q was previously shown to exhibit a depolarized shift in voltage dependence of inactivation and slowed onset of inactivation compared with WT channels (Berecki et al., 2018; Mason et al., 2019). However, none of the variants have been studied in the two splice isoforms. We demonstrate that $Na_V1.2$ variants associated with EOEE exhibit greater dysfunction when expressed in the neonatal splice proteoform. Our results indicate that both developmentally regulated alternative mRNA splicing of $Na_V1.2$ and developmental stage are important factors promoting neuronal hyperexcitability. These observations have implications for understanding the pathophysiology of EOEE and for guiding experimental strategies to determine the functional consequences of Na_V channel variants associated with these life-threatening, early-life neurodevelopmental disorders.

Materials and methods

Mutagenesis and heterologous expression of $Na_V1.2$

Mutagenesis of recombinant human $Na_V1.2$ was performed as described previously (Lossin et al., 2002; Rhodes et al., 2004; Kahlig et al., 2008; Thompson et al., 2011). To generate the neonatal splice isoform ($Na_V1.2N$), a single substitution (D209N) was introduced. Five EOEE-associated variants (T236S, E999K, S1336Y, T1623N, and R1882Q) were introduced into both $Na_V1.2N$ and $Na_V1.2A$ splice isoforms. To minimize spontaneous mutagenesis of $Na_V1.2$ cDNA in bacteria, recombinants were always propagated in Stbl2 cells (Invitrogen) at 30°C.

Heterologous expression of WT or $Na_V1.2$ variants was performed in tsA201 cells. Heterologous expression in tsA201 cells was chosen for these experiments to enable precise measurement of biophysical parameters associated with WT or mutant $Na_V1.2$ channels, without the contamination of other sodium currents that may be found in native neuronal cells. Cells were grown in 5% CO_2 at 37°C in Dulbecco's modified Eagle's medium supplemented with 10% FBS, 2 mM L-glutamine, 50 units/ml penicillin, and 50 µg/ml streptomycin. Cells were transiently cotransfected with $Na_V1.2$ and the accessory β_1 and β_2 subunits (2 µg total plasmid DNA was transfected with a cDNA ratio of 10:1:1 for $Na_V1.2$:β_1:β_2 subunits) using SuperFect reagent (Qiagen). Human β_1 and β_2 cDNAs were cloned into plasmids encoding the CD8 receptor (CD8-IRES-hβ_1) or enhanced GFP-IRES-hβ_2, respectively, as transfection markers, as previously described.

Voltage-clamp recording and data analysis

Whole-cell voltage clamp experiments of heterologous cells were performed as previously described (Thompson et al., 2011, 2012). Whole-cell voltage-clamp recordings were made at room temperature using an Axopatch 200B amplifier (Molecular Devices). Patch pipettes were pulled from borosilicate glass capillaries (Harvard Apparatus) with a multistage P-1000 Flaming-Brown micropipette puller (Sutter Instruments) and fire-polished using a microforge (Narashige MF-830) to a resistance of 1.5–2.5 MΩ. The pipette solution consisted of (in mM): 10 NaF, 105 CsF, 20 CsCl, 2 EGTA, and 10 HEPES, with pH adjusted to 7.35 with CsOH and osmolality adjusted to 300 mOsmol/kg with sucrose. The recording solution was continuously perfused with bath solution containing (in mM): 145 NaCl, 4 KCl, 1.8 $CaCl_2$, 1 $MgCl_2$, 10 glucose, and 10 HEPES, with pH 7.35 and osmolality 310 mOsmol/kg. The reference electrode consisted of a 2% agar bridge with composition similar to the bath solution. All chemicals were purchased from Sigma-Aldrich.

Voltage-clamp pulse generation and data collection were done using Clampex 10.4 (Molecular Devices). Whole-cell capacitance was determined by integrating capacitive transients generated by a voltage step from −120 mV to −110 mV filtered at 100 kHz low-pass Bessel filtering. Series resistance was compensated with prediction >70% and correction >90% to ensure that the command potential was reached within microseconds with a voltage error <3 mV. Leak currents were subtracted by using an online P/4 procedure. All whole-cell currents were filtered at 5 kHz low-pass Bessel filtering and digitized at 50 kHz. All voltage-clamp experiments were conducted at room temperature (20–25°C).

Data were analyzed using a combination of Clampfit 10.4 (Molecular Devices), Excel 2013 (Microsoft), and SigmaPlot 12.5 (Systat Software). Peak current was normalized for cell capacitance and plotted against step voltage to generate a peak current density–voltage relationship. Whole-cell conductance (G_{Na}) was calculated as $G_{Na} = I/(V - E_{rev})$, where I is the measured peak current, V is the step potential, and E_{rev} is the calculated sodium reversal potential. G_{Na} at each voltage step was normalized to the maximum conductance between −80 mV and 20 mV. To calculate voltage dependence of activation (protocol described in figure insets), normalized G_{Na} was plotted against voltage and fitted with the Boltzmann function $G/G_{max} = (1 + \exp[(V - V_{1/2})/k])^{-1}$, where $V_{1/2}$ indicates the voltage at half-maximal activation, and k is a slope factor describing voltage sensitivity of the channel. Voltage dependence of steady-state inactivation was assessed by plotting currents generated by the −10-mV postpulse voltage step normalized to the maximum current against prepulse voltage step from −140 to −10 mV in 10-mV increments. The plot was fitted with the Boltzmann function. Time-dependent recovery from inactivation was evaluated by fitting peak current recovery with a two-exponential function. Chord

conductance at 0 mV (20 trials from a holding potential of −120 mV) was determined using non-stationary fluctuation analysis where $\sigma^2(I) - iI - (I^2/N)$, where σ^2 is variance, i is single-channel current, I is average current, and N is number of channels.

Results are presented as mean ± SEM. The statistical tests performed are specified in the figure legends. $P < 0.05$ was considered statistically significant.

Computational modeling

Simulations were performed using a pyramidal cell model in the NEURON environment, as previously described (Schmidt-Hieber and Bischofberger, 2010; Hallermann et al., 2012; Ben-Shalom et al., 2017; Spratt et al., 2019). All EOEE syndrome variants were modeled as changes relative to this baseline. All Na_V channel simulations were performed at 25°C to match recording conditions. All neuronal simulations were performed at 33°C, with kinetics scaled by the Q_{10} factor within the model. Because changes in whole-cell current densities may be a by-product of expression system, we only modeled changes in sodium channel biophysical parameters. All neuronal simulations assumed heterozygosity. Model files will be provided upon request to the author.

Results

Developmentally regulated alternative mRNA splicing is a conserved feature of human Na_V channels. In human $Na_V1.2$, alternative splicing involves a pair of mutually exclusive exons encoding part of S3 and S4 in domain I and generates two channel proteoforms (designated $Na_V1.2$-neonatal [$Na_V1.2N$] and $Na_V1.2$-adult [$Na_V1.2A$]) that differ by a single amino acid residue (adult to neonatal: D209N, Fig. 1 A). We compared the functional properties of heterologously expressed WT $Na_V1.2N$ and $Na_V1.2A$ proteoforms. Total whole-cell current density, voltage dependence of channel inactivation, and recovery from fast inactivation were not significantly different between the two WT $Na_V1.2$ proteoforms (Fig. 1). However, $Na_V1.2N$ exhibited a significantly depolarized voltage dependence of activation compared with $Na_V1.2A$ (activation $V_{1/2}$: WT-$Na_V1.2N$, −19.6 ± 0.8 mV; $Na_V1.2A$, −23.5 ± 1.3 mV, $n = 15$; $P = 0.0172$; Fig. 1 D). This depolarized voltage dependence of activation may limit neuronal excitability during early development (Xu et al., 2007; Gazina et al., 2015).

Biophysical properties of epileptic encephalopathy–associated $Na_V1.2$ variants

We investigated the functional consequences of five EOEE-associated $Na_V1.2$ variants. Four variants, reported originally by Nakamura et al. (2013), were identified in neonates having seizures associated with a suppression-burst EEG pattern beginning within the first week of life (age 0–1 d for three variants, age 6 d for E999K). Three of the subjects were described as having medically intractable epilepsy (an exception was the carrier of T236S, who responded to a four-antiepileptic-drug regimen), and all had severe developmental delay. The initial diagnosis was Ohtahara syndrome in all cases, but three were later reclassified as West syndrome due to emergence of hypsarrhythmia on EEG. The other variant, R1882Q, is recurrent and presents with focal seizures on the first day of life that evolves to severe developmental delay (Howell et al., 2015). These variants were specifically chosen because the associated clinical phenotypes had very early onset, and they were also chosen to represent each domain of the sodium channel.

We first examined whole-cell sodium current density for WT and mutant $Na_V1.2N$. Current density for $Na_V1.2N$-E999K, $Na_V1.2N$-T1623N, and $Na_V1.2N$-R1882Q was not statistically different from WT. However, T236S expressed in $Na_V1.2N$ had approximately twofold larger currents than the WT channel ($Na_V1.2N$-WT: −480.9 ± 60.9 pA/pF, $n = 15$; $Na_V1.2N$-T236S: −985.9 ± 184.8 pA/pF, $n = 15$, $P = 0.0037$; Fig. 2, B and C; and Fig. 3). We calculated chord conductance at 0 mV using non-stationary fluctuation analysis and found no difference between NaV1.2N-WT and NaV1.2N-T236S (19.9 ± 4.4 vs. 23.4 ± 3.4 pS, respectively, $n = 5$ each, $P = 0.75$). Also, we observed a strong trend toward smaller current density compared with WT $Na_V1.2N$ for $Na_V1.2N$-S1336Y (−113.7 ± 26.9 pA/pF, $n = 10$, $P = 0.0549$). Similar to that of the neonatal isoform, neither $Na_V1.2A$-E999K, $Na_V1.2A$-$Na_V1.2A$-T1623N, nor $Na_V1.2A$-R1882Q showed any alterations in current density. The $Na_V1.2A$-S1336Y variant showed similarly small currents compared with the neonatal isoform of the channel (−104.7 ± 14.7 pA/pF, $n = 11$, $P = 0.0045$; Fig. 2, B and C; and Fig. 3). However, the larger current density observed for $Na_V1.2N$-T236S was not evident in the adult isoform (WT $Na_V1.2A$: −518.4 ± 50.9 pA/pF, $n = 15$; $Na_V1.2A$-T236S: −405.2 ± 83.9 pA/pF, $n = 9$, $P = 0.87$; Fig. 2, B and C; and Fig. 3).

We determined if the variants altered the voltage dependence of channel activation. We observed that $Na_V1.2N$-T236S, $Na_V1.2N$-E999K, and $Na_V1.2N$-S1336Y all had hyperpolarized voltage dependence of activation compared with WT $Na_V1.2N$ ($Na_V1.2N$: −19.6 ± 0.8 mV, $n = 15$; $Na_V1.2N$-T236S: −29.9 ± 1.1 mV, $n = 15$, $P < 0.0001$; $Na_V1.2N$-E999K: −26.7 ± 1.7 mV, $n = 14$, $P = 0.003$; $Na_V1.2N$-S1336Y: −25.3 ± 1.9 mV, $n = 10$, $P = 0.0278$; Fig. 4 and Table 1). However, when voltage dependence of activation was measured in the adult isoform, we found that the mutants were indistinguishable from WT $Na_V1.2A$ (WT-$Na_V1.2A$: −23.5 ± 1.3 mV, $n = 15$; $Na_V1.2A$-T236S: −25.6 ± 2.0 mV, $n = 9$, $P = 0.78$; $Na_V1.2A$-E999K: −24.6 ± 1.4 mV, $n = 10$, $P = 0.96$; $Na_V1.2A$-S1336Y: −23.2 ± 1.4 mV, $n = 11$, $P = 0.99$; Fig. 4 and Table 1). Interestingly, in $Na_V1.2A$, we observed a depolarized shift in the voltage dependence of activation for T1623N (−18.4 ± 1.4 mV, $n = 8$, $P = 0.0316$; Fig. 4 and Table 1). These results suggest that three variants, T236S, E999K, and S1336Y, may confer neuronal hyperexcitability, but only when expressed in $Na_V1.2N$.

We investigated whether the variants exhibited a compensatory hyperpolarization in the voltage dependence of inactivation when expressed in $Na_V1.2N$. We found that both T236S and E999K were indistinguishable from WT $Na_V1.2N$ (WT-$Na_V1.2N$: −62.4 ± 1.2 mV, $n = 15$; $Na_V1.2N$-T236S: −62.3 ± 0.8 mV, $n = 8$, $P = 0.999$; $Na_V1.2N$-E999K: −63.1 ± 1.3 mV, $n = 13$, $P = 0.992$; Fig. 5 and Table 1). However, $Na_V1.2N$-S1336Y, $Na_V1.2N$-T1623N, and $Na_V1.2N$-R1882Q all showed a depolarized shift in the voltage dependence of inactivation ($Na_V1.2N$-S1336Y: −56.9 ± 1.0 mV, $n = 10$, $P = 0.0075$; $Na_V1.2N$-T1623N: −56.3 ± 0.7 mV, $n = 9$,

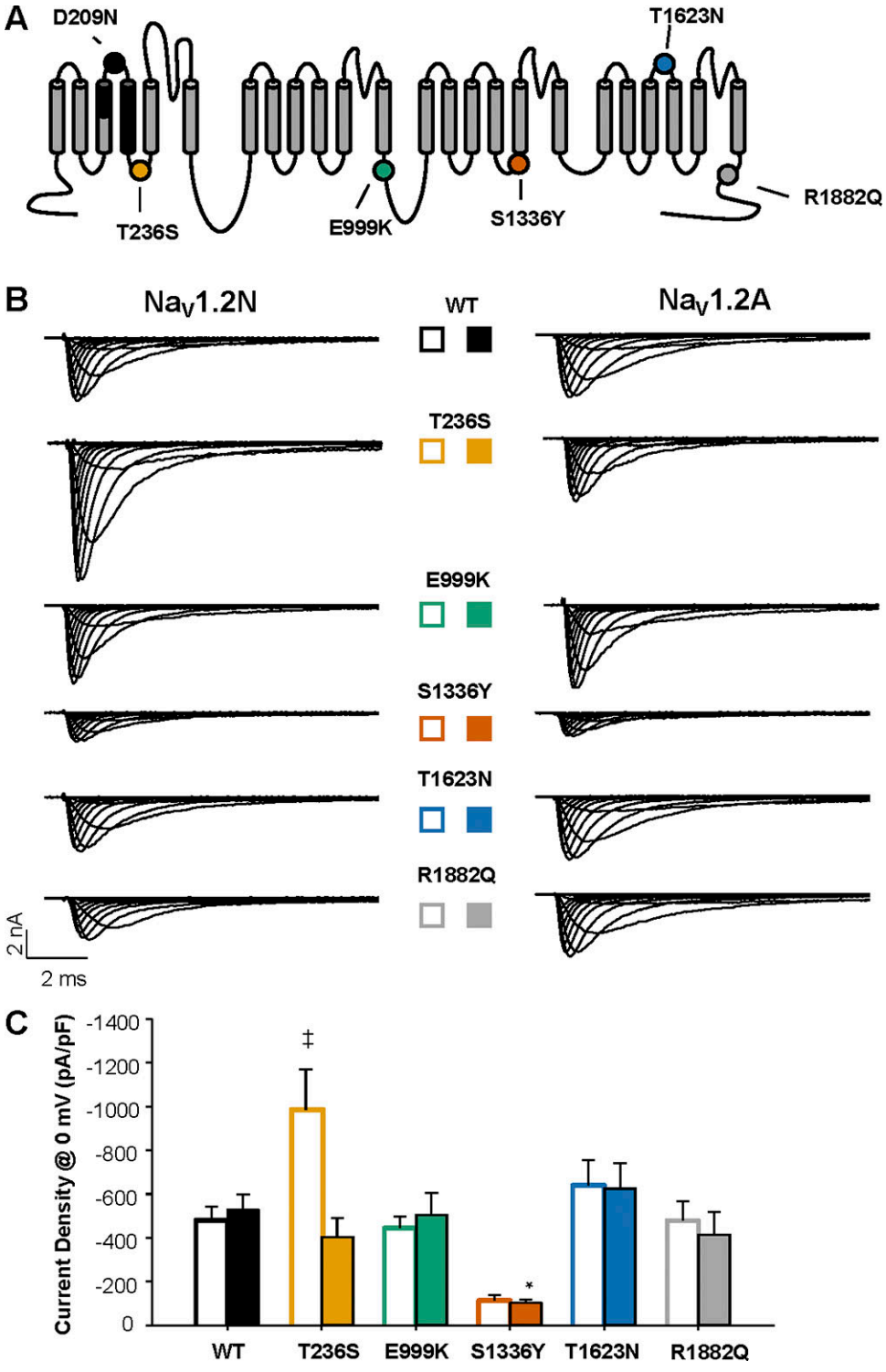

Figure 2. **Function of EOEE-associated variants. (A)** Predicted transmembrane topology of Na$_V$1.2, highlighting the location of the exon 5 coding region (black shaded), amino acid change associated with alternative exon splicing (black dot), and EOEE-associated variants (colored dots). **(B)** Whole-cell sodium currents of EOEE-associated Na$_V$1.2 variants in either the adult (Na$_V$1.2N; left) or neonatal (Na$_V$1.2A; right) splice isoforms. **(C)** Peak current density elicited by test pulses to 0 mV from a holding potential of −120 mV for Na$_V$1.2N (open bars) and Na$_V$1.2A (closed bars) proteoforms. All data are expressed as mean ± SEM for 8–15 measurements. *, $P < 0.05$ compared with Na$_V$1.2A; ‡, $P < 0.05$ Na$_V$1.2N. EOEE-associated variants were compared with WT Na$_V$1.2 of the same proteoform using a one-way ANOVA, followed by Dunnett's post hoc test.

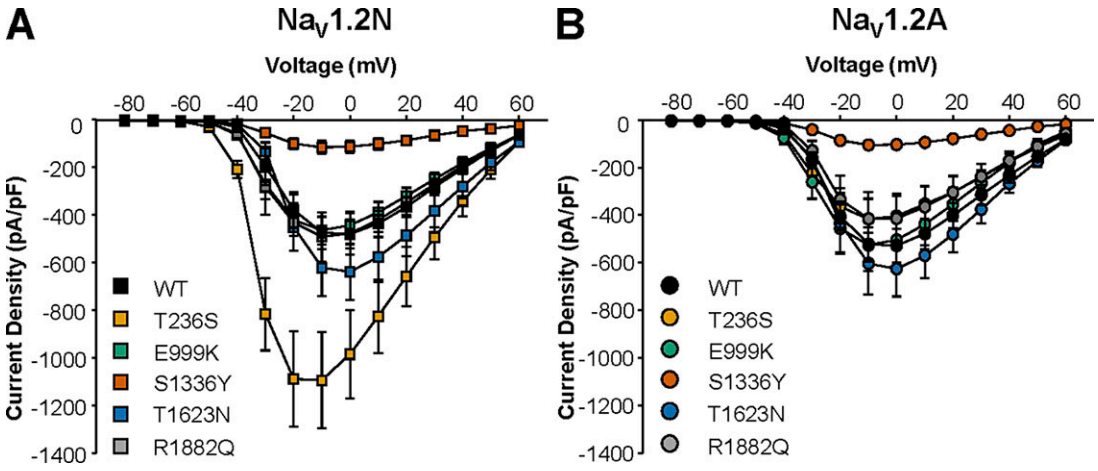

Figure 3. **The impact of $Na_V1.2$ alternative splicing on sodium current density. (A and B)** Current–voltage relationships for WT and EOEE-associated variants expressed in the neonatal (A) or adult (B) $Na_V1.2$ splice isoforms. All data are expressed as mean ± SEM for 8–15 measurements.

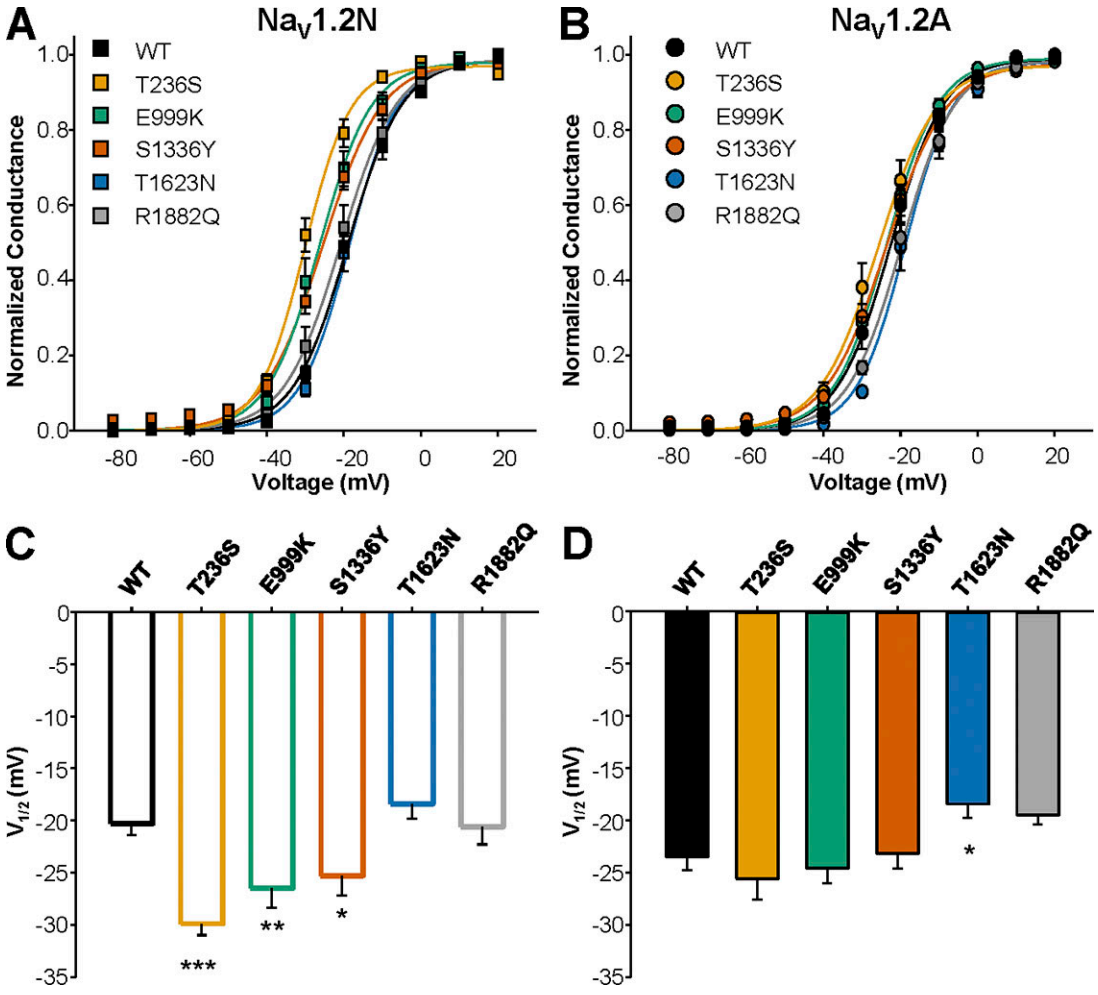

Figure 4. **Alternative splicing of $Na_V1.2$ differentially modulates the effect of EOEE-associated variants on channel activation. (A and B)** Voltage dependence of activation for WT and EOEE-associated $Na_V1.2$ variants in the neonatal (A) or adult (B) proteoform. **(C and D)** Values for $V_{1/2}$ of activation for WT and EOEE-associated $Na_V1.2$ variants in the neonatal (C) or adult (D) proteoform. All data are expressed as mean ± SEM for 8–15 measurements. EOEE-associated variants were compared with WT $Na_V1.2$ of the same proteoform using one-way ANOVA, followed by Dunnett's post hoc test. ***, $P < 0.0001$; **, $P < 0.01$; *, $P < 0.05$.

Table 1. **Biophysical properties of $Na_V1.2$ variants**

Variant	Voltage dependence of activation			Voltage dependence of fast inactivation			Recovery from fast inactivation (−10 mV)		
	$V_{1/2}$ (mV)	k (mV)	*n*	$V_{1/2}$ (mV)	k (mV)	*n*	τ_f (ms) (amplitude)	τ_s (ms) (amplitude)	*n*
$Na_V1.2A$	−23.5 ± 1.3	6.3 ± 0.3	15	−63.5 ± 0.9	−6.2 ± 0.1	15	1.9 ± 0.1 (0.90 ± 0.01)	275.6 ± 16.4 (0.12 ± 0.01)	15
$Na_V1.2A$-T236S	−25.6 ± 2.0	7.0 ± 0.3	9	−65.3 ± 1.8	−5.6 ± 0.1	9	2.1 ± 0.1 (0.87 ± 0.01)	270.1 ± 16.8 (0.14 ± 0.01)	8
$Na_V1.2A$-E999K	−4.6 ± 1.4	6.5 ± 0.3	10	−63.1 ± 1.2	−6.2 ± 0.1	10	1.9 ± 0.2 (0.90 ± 0.01)	269.3 ± 21.2 (0.14 ± 0.01)	10
$Na_V1.2A$-S1336Y	−23.2 ± 1.4	7.9 ± 0.4	11	−57.7 ± 1.3[a]	−6.6 ± 0.3	11	1.3 ± 0.2 (0.84 ± 0.03)	210.3 ± 20.4 (0.21 ± 0.02)	11
$Na_V1.2A$-T1623N	−18.4 ± 1.4[a]	6.4 ± 0.6	8	−56.7 ± 0.8[a]	−6.0 ± 0.1	8	2.1 ± 0.1 (0.92 ± 0.01)	240.4 ± 17.4 (0.09 ± 0.01)	8
$Na_V1.2A$-R1882Q	−19.5 ± 0.9	6.7 ± 0.3	15	−51.2 ± 1.5[a]	−7.6 ± 0.3[a]	15	1.6 ± 0.1 (0.84 ± 0.02)	248.2 ± 22.0 (0.16 ± 0.02)	15
$Na_V1.2N$	−19.5 ± 0.8[b]	7.0 ± 0.3	15	−62.4 ± 1.2	−6.4 ± 0.1	15	1.7± 0.1 (0.90 ± 0.01)	267.3 ± 28.8 (0.13 ± 0.01)	15
$Na_V1.2N$-T236S	−29.9 ± 1.1[a]	5.7 ± 0.4[a]	15	−62.3 ± 0.8	6.1 ± 0.4	8	1.9 ± 0.1 (0.87 ± 0.01)	245.3 ± 7.7 (0.14 ± 0.01)	7
$Na_V1.2N$-E999K	−26.2 ± 1.7[a]	6.3 ± 0.4	14	−63.1 ± 1.3	−5.8 ± 0.1	13	1.8 ± 0.1 (0.89 ± 0.01)	263.2 ± 22.9 (0.12 ± 0.01)	13
$Na_V1.2N$-S1336Y	−25.3 ± 1.9[a]	7.3 ± 0.7	10	−56.9 ± 1.0[a]	−7.9 ± 0.8[a]	10	1.0 ± 0.1 (0.89 ± 0.02)	261.0 ± 38.8 (0.16 ± 0.03)	10
$Na_V1.2N$-T1623N	−18.4 ± 1.4	6.2 ± 0.3	9	−56.3 ± 0.7[a]	−6.3 ± 0.4	9	2.0 ± 0.1 (0.87 ± 0.02)	213.6 ± 23.9 (0.14 ± 0.02)	9
$Na_V1.2N$-R1882Q	−20.6 ± 1.7	6.2 ± 0.4	14	−53.4 ± 1.3[a]	−7.0 ± 0.2[a]	14	1.6 ± 0.1 (0.88 ± 0.02)	258.2 ± 27.8 (0.12 ± 0.02)	14

[a]P < 0.05 between WT and variant in same splice isoform.
[b]P < 0.05 between neonatal and adult isoforms.

P = 0.0049; $Na_V1.2N$-R1882Q: −53.4 ± 1.3 mV, *n* = 14, P < 0.0001; Fig. 5, A and C; and Table 1). These differences in voltage dependence of inactivation were proteoform independent, with similar depolarized shifts observed in $Na_V1.2A$ (WT-$Na_V1.2A$: −63.5 ± 0.9 mV, *n* = 15; $Na_V1.2A$-S1336Y: −57.7 ± 1.3 mV, *n* = 11, P = 0.0011; $Na_V1.2A$-T1623N: −56.7 ± 0.8 mV, *n* = 8, P = 0.0055; $Na_V1.2A$-R1882Q: −51.2 ± 1.5 mV, *n* = 14, P < 0.0001; Fig. 5, B and D; and Table 1).

The kinetics of inactivation (Fig. 6, A and B) and recovery from inactivation (Fig. 6, C and D) were indistinguishable between WT and most of the mutant channels regardless of the channel proteoform (Fig. 6 and Table 1). However, both T1623N and R1882Q exhibited a significantly slower entry into the fast inactivated state, as evidenced by the larger time constant for inactivation across a range of voltages in both $Na_V1.2N$ and $Na_V1.2A$ (Fig. 6, A and B).

Integrating and interpreting functional effects of $Na_V1.2$ variants

Missense variation in $Na_V1.2$ can result in complex changes to channel functional properties. As a result, it can be difficult to understand how these changes sum to a net gain or loss of channel function. To better summarize and integrate the functional differences among channel variants and alternatively spliced proteoforms, we constructed radar plots incorporating peak sodium current density, voltage dependence of activation and inactivation, and the kinetics of inactivation, relative to the WT channel. By plotting the data together, we could better interpret the net effect of a variant on overall channel function. We configured each radar spoke such that points lying outside of the WT plot would be indicative of a gain of function, while points lying within the WT plot would indicate loss of function.

As illustrated in Fig. 7, all five EOEE-associated mutations showed significant deviations from WT channels in $Na_V1.2N$. Most effects observed in the $Na_V1.2N$ background were consistent with gain of function, whereas one mutation (S1336Y) exhibited a mixture of gain- and loss-of-function defects. However, in the $Na_V1.2A$ background, the differences in voltage dependence of activation were absent for T236S, E999K, and S13336Y, but the overt differences in voltage dependence of inactivation were present for S1336Y, T1623N, and R1882Q.

Computational modeling of EOEE-associated $Na_V1.2$ variants

To evaluate how $Na_V1.2$ dysfunction affects neuronal excitability, we incorporated the functional properties of each mutation into an established computational model of a cortical pyramidal neuron (Hallermann et al., 2012; Ben-Shalom et al., 2017). We created computational models to simulate sodium currents conducted by $Na_V1.2A$ or $Na_V1.2N$, as well as each mutant channel, in both proteoforms. Our models successfully recapitulated the functional differences observed between $Na_V1.2A$ and $Na_V1.2N$ (Fig. 8, A and B), as well the biophysical properties of all mutations (Fig. 8 C). Importantly, because whole-cell current density is highly variable and may be dependent on cell type, we only modeled changes in voltage-dependent activation and inactivation along with kinetic parameters. For comparison, we modeled the benign familial neonatal-infantile seizures (BFNIS) associated $Na_V1.2$ mutation L1563V, using previously published data (Fig. 8 C; Xu et al., 2007). This mutation has been shown to exhibit biophysical properties that are dependent on splice isoform.

To recapitulate the neuronal environment at different developmental stages, we performed simulations incorporating $Na_V1.2A$ and $Na_V1.2N$ at specific ratios based on published data from mouse brain (Gazina et al., 2010). To simulate an immature

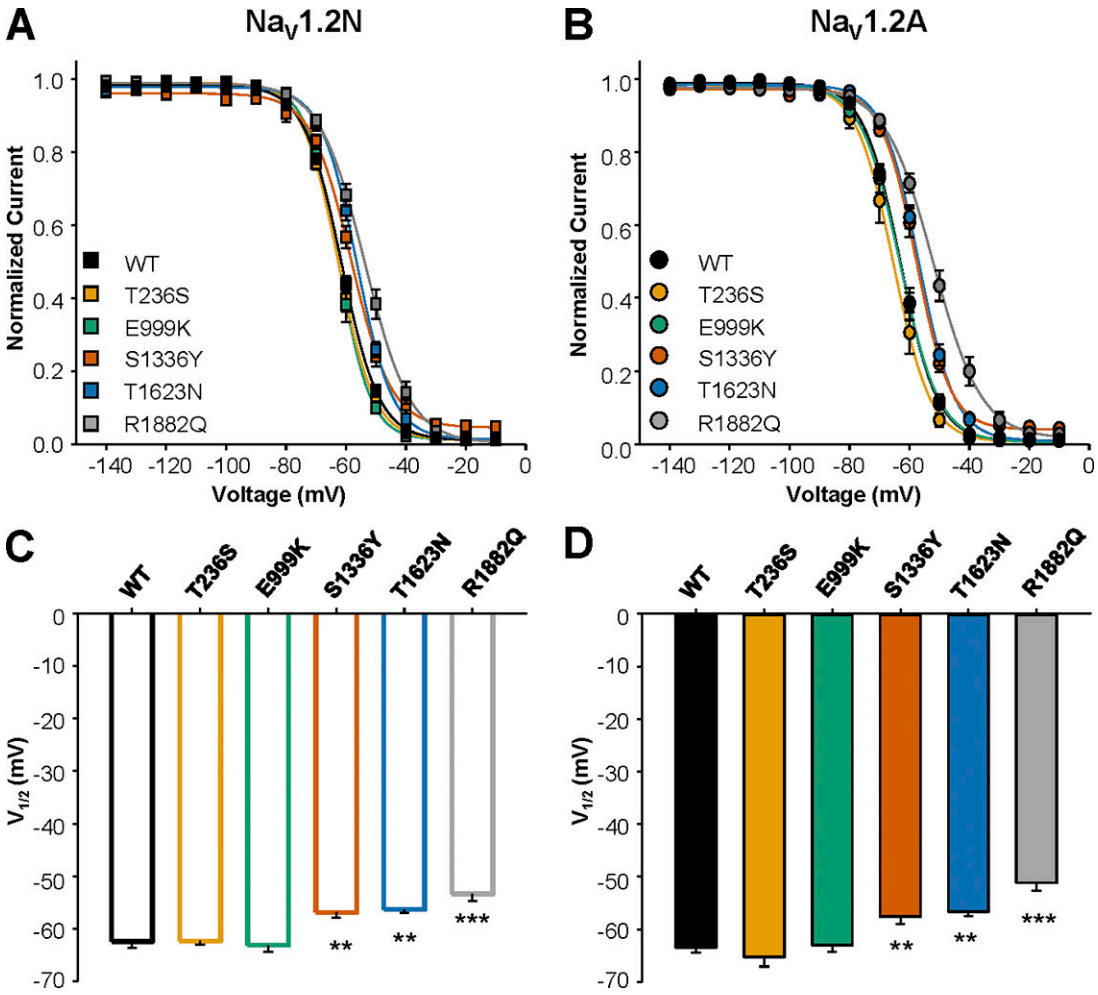

Figure 5. **Voltage dependence of inactivation of EOEE-associated Na$_V$1.2 variants. (A and B)** Voltage dependence of inactivation for WT and EOEE-associated Na$_V$1.2 variants in the neonatal (A) or adult (B) proteoform. **(C and D)** Values for $V_{1/2}$ of inactivation for WT and EOEE-associated Na$_V$1.2 variants in the neonatal (C) or adult (D) proteoform. All data are expressed as mean ± SEM for 8–15 measurements. EOEE-associated variants were compared with WT Na$_V$1.2 of the same proteoform using one-way ANOVA, followed by Dunnett's post hoc test. ***, P < 0.0001; **, P < 0.01.

neuron, we developed a model expressing 67% Na$_V$1.2N and 33% Na$_V$1.2A. Simulations of the WT channels in this model showed that expression of 100% WT Na$_V$1.2N or a mixture of Na$_V$1.2A and Na$_V$1.2N was associated with lower neuronal excitability compared with neurons expressing 100% WT Na$_V$1.2A (Fig. 9). Therefore, while the ∼3-mV difference in voltage dependence of activation between Na$_V$1.2N and Na$_V$1.2A may appear small, it is sufficient to affect excitability. This is similar to predictions made by other neuronal models, which demonstrate that Na$_V$1.2N-expressing neurons have lower excitability compared with neurons expressing WT channels (Xu et al., 2007). However, when we incorporated each EOEE-associated Na$_V$1.2 mutation into the immature neuron model with a mixture of Na$_V$1.2A and Na$_V$1.2N, all but one (T1623N) exhibited overtly greater neuronal excitability (Fig. 10, A and B). We additionally modeled Na$_V$1.2-L1563V, a mutation associated with BFNIS. This mutation evoked a modest enhancement of excitability compared with WT neurons but was not as excitable as most EOEE-associated mutations (Fig. 10, A and B). Interestingly, although R1882Q is associated with EOEE, it also exhibited a small enhancement of excitability in immature neurons (Fig. 10, A and B). This suggests that five of these six mutations exert gain-of-function effects strong enough to overcome the normally dampening effect of the Na$_V$1.2N on neuronal excitability.

As discussed above, patients with Na$_V$1.2-associated EOEE often present symptoms within the first days of life (Nakamura et al., 2013). Previous work has shown that potassium conductance is significantly smaller in mouse neocortical pyramidal neurons immediately after birth and steadily rises during the first weeks of life (Guan et al., 2011). Because we observed relatively mild phenotypes for two EE-associated mutations, T1623N and R1882Q, we hypothesized that a more overt phenotype may be observed at an earlier developmental time point when lower potassium conductance may predispose to hyperexcitability.

To determine the impact of EOEE-associated Na$_V$1.2 variants on neuronal excitability in simulated neonatal neurons, we reduced the potassium channel conductance to one-third of that used for the immature neuron described above, while maintaining the sodium channel ratio of 67% Na$_V$1.2N and 33%

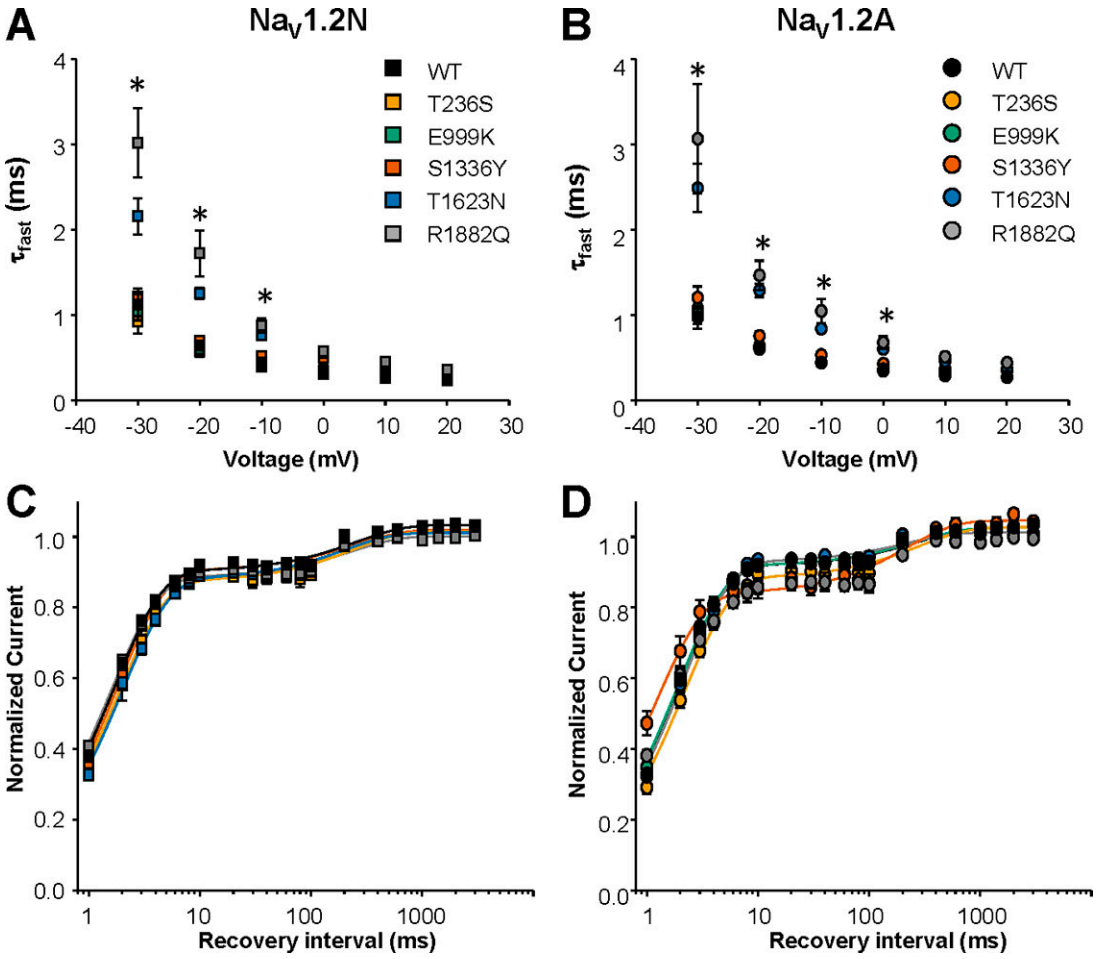

Figure 6. **Alternative $Na_V1.2$ splicing does not impact the effect of EOEE-associated variants on the kinetics of fast inactivation. (A and B)** Voltage dependence of time constants for the onset of fast inactivation for WT and EOEE associated $Na_V1.2$ variants in the $Na_V1.2N$ (A) and $Na_V1.2A$ (B) isoforms. All data are expressed as mean ± SEM for 8–15 measurements. **(C and D)** Recovery from fast inactivation for WT and EOEE-associated $Na_V1.2$ variants in the neonatal (C) and adult (D) isoforms. All data are expressed as mean ± SEM for 8–15 measurements. EOEE-associated variants were compared with WT $Na_V1.2$ of the same proteoform using one-way ANOVA, followed by Dunnett's post hoc test. *, $P < 0.05$.

$Na_V1.2A$ (Fig. 10). Interestingly, neurons bearing either T236S or E999K, which exhibit large hyperpolarized shifts in the voltage dependence of activation, and S1336Y, which has hyperpolarized activation and depolarized inactivation, were either in a perpetual state of depolarization block (T236S and S1336Y) or entered into depolarization block more readily than WT neurons (E999K; Fig. 10, A and C). The mutations T1623N and R1882Q, which showed only modest effects on excitability with the full potassium current, showed greater excitability in the neonatal neuron model, being resistant to depolarization block compared with a WT neuron, while the BFNIS mutation exhibited only a modest enhancement of excitability (Fig. 10 C).

To simulate a mature neuron, we used a published model that restricts $Na_V1.2$ expression to the proximal AIS and incorporates $Na_V1.6$ into the distal AIS and nodes of Ranvier (Ben-Shalom et al., 2017). In the mature neuron model, $Na_V1.2$ was represented as 33% $Na_V1.2N$ and 67% $Na_V1.2A$. Simulations with WT channels showed that neuronal excitability was not different when 100% $Na_V1.2N$, 100% $Na_V1.2A$, or a mixture were present (Fig. 10 B). Further, mature neurons expressing each of the six variants exhibited minor differences in neuronal excitability (Fig. 10, A and D). Thus, differences in excitability among WT and mutant neurons depend greatly on the developmental context in which those variants are expressed, with hyperexcitability being exacerbated in immature developing neurons (Fig. 10). Thus, these results predict that the functional effects of EOEE-associated $Na_V1.2$ variants will have the greatest impact on neuronal excitability in immature or neonatal neurons, which is consistent with the very early onset of these epilepsies.

Discussion

Variants in multiple Na_V channel genes are associated with clinically diverse genetic epilepsies and neurodevelopmental disorders. Investigations of the functional consequences of various Na_V channel variants have revealed fundamental mechanistic information implicating $Na_V1.1$ loss of function in the pathogenesis of Dravet syndrome, and $Na_V1.6$ gain of function as a cause for many cases of *SCN8A* epileptic encephalopathy (Yu et al., 2006; Ogiwara et al., 2007; Estacion et al., 2014;

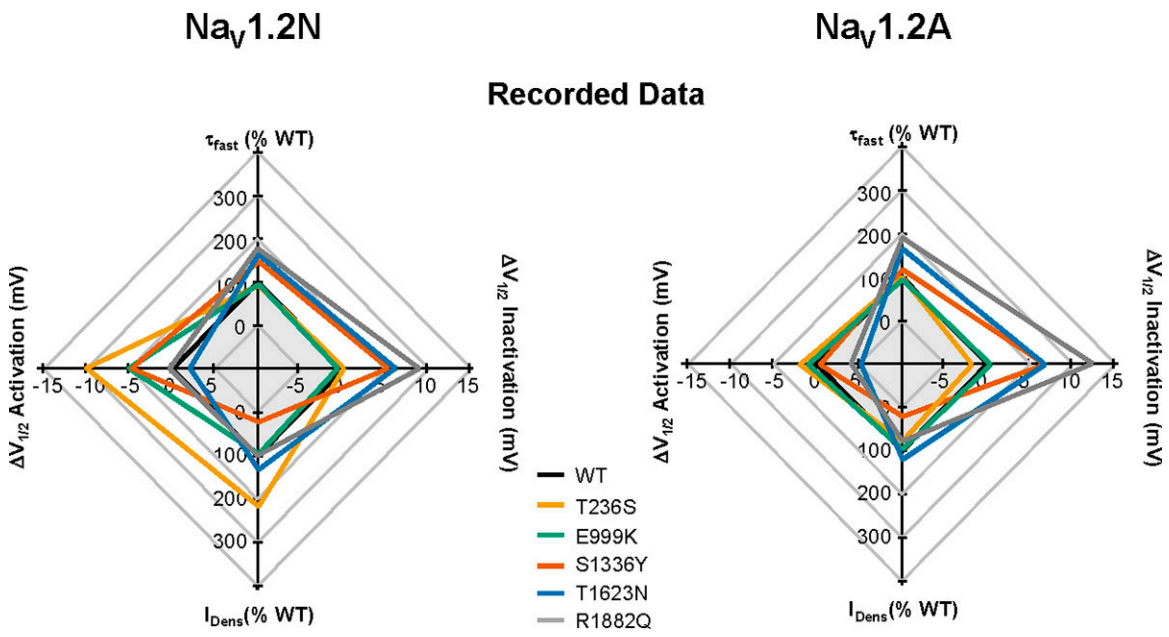

Figure 7. **Radar plots illustrating differences in functional consequences of Na$_V$1.2 variants.** Plots were constructed with each spoke arranged such that points lying outside of the WT plot would be indicative of a gain of function, while points lying within the WT plot would indicate a loss of function. The effects of each mutant channel relative to WT are illustrated for Na$_V$1.2N (left) and Na$_V$1.2A (right) from experimentally collected data.

Wagnon et al., 2015; Lopez-Santiago et al., 2017). Functional studies have demonstrated a bifurcated pathophysiology of epilepsy and neurodevelopmental disorders associated with *SCN2A* variants. Specifically, Na$_V$1.2 gain of function appears typical of EOEE, whereas loss of function seems more prevalent among variants associated with autism spectrum disorder or later-onset epilepsy, although there is significant comorbidity associated with autism spectrum disorders and epilepsy (Ben-Shalom et al., 2017). However, the fundamental reason for early-onset epilepsy in the setting of *SCN2A* mutation is not completely understood.

In this study, we investigated the contribution of a developmentally regulated alternative mRNA splicing event to the pathogenesis of *SCN2A*-associated epileptic encephalopathy. Previous studies have demonstrated that alternative splicing of *SCN1A*, *SCN2A*, *SCN5A*, and *SCN9A* have important effects on the functional and pharmacological properties of WT and mutant channels encoded by these genes (Kasai et al., 2001; Copley, 2004; Diss et al., 2004; Onkal et al., 2008; Thompson et al., 2011). With respect to *SCN2A*, there are functional differences between the two developmentally regulated alternatively spliced Na$_V$1.2 isoforms, which may have physiological relevance. The neonatal-expressed Na$_V$1.2N exhibits a depolarized voltage dependence of activation (Fig. 1), and this may dampen excitability in developing neurons.

Our results contrast with previous work that examined functional difference for Na$_V$1.2N and Na$_V$1.2A proteoforms (Xu et al., 2007). The prior work showed that Na$_V$1.2N exhibited faster onset of inactivation and hyperpolarized voltage-dependent inactivation compared with Na$_V$1.2A, while we observed only a depolarized shift in activation for Na$_V$1.2N. One factor that may explain these differences is the coexpression of β1 and β2 subunits in our study. The β subunits have been shown to alter sodium channel biophysical properties and trafficking (Isom et al., 1992, 1995; Chen et al., 2002; Uebachs et al., 2010). However, both studies concur that the net effect of Na$_V$1.2N biophysical properties predicts blunted neuronal excitability. This notion is supported by a previous study of mice engineered to express only Na$_V$1.2A that demonstrated greater cortical pyramidal neuronal excitability beginning at postnatal day 3 (P3), and greater susceptibility to pentylenetetrazole-induced seizures beginning at P3 that persisted into adulthood (P53–P75; Gazina et al., 2015). Further, our demonstration that incorporating Na$_V$1.2N into a compartmental model of a developing cortical pyramidal neuron results in lower firing frequency than neuron models incorporating only the adult proteoform (Fig. 9) also supports the relevance of *SCN2A* alternative splicing.

Given its physiological importance during early development, we investigated the impact of alternative splicing on a set of EOEE-associated *SCN2A* variants. We tested the hypothesis that the functional consequences of EOEE-associated Na$_V$1.2 variants are potentiated in Na$_V$1.2N, a phenomenon that may contribute to the early age of onset. The five Na$_V$1.2 variants we studied exhibited mostly gain-of-function effects in Na$_V$1.2N, but the functional consequences of these variants were more muted when expressed in the context of canonical Na$_V$1.2A (adult expressed). Specifically, when expressed in Na$_V$1.2N, three of the variants showed greater hyperpolarizing shifts in voltage dependence of activation, while one variant was protected from a depolarizing shift in voltage dependence of inactivation. Given that the splicing event involves a switch of the domain 1 voltage sensor, it is possible that variants with significant shifts in voltage dependence of activation may be

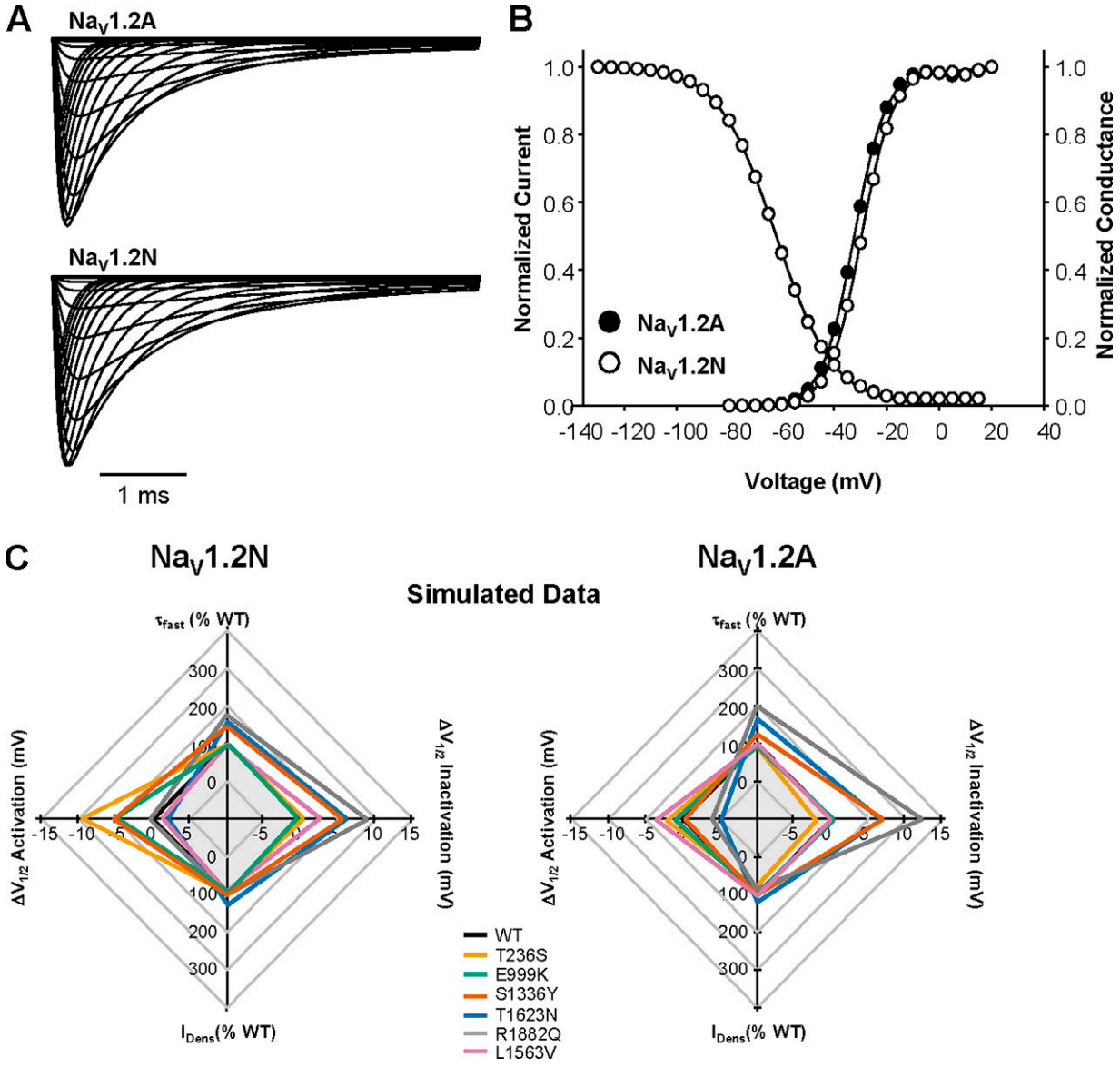

Figure 8. **Computational modeling of WT Na$_V$1.2 splice isoforms. (A)** Simulated whole-cell sodium current for Na$_V$1.2A (top) and Na$_V$1.2N (bottom). **(B)** Voltage dependence of activation and inactivation for simulated sodium currents mediated by the Na$_V$1.2N (open circles) and Na$_V$1.2A (closed circles). Curves for voltage dependence of inactivation for both isoforms are superimposed. **(C)** Radar plots comparing changes in biophysical parameters of whole-cell sodium current from simulated data for Na$_V$1.2N (left) and Na$_V$1.2A (right).

disproportionately affected by this alternative splicing event. For Na$_V$1.2N-T236S, given no change in single-channel conductance, the increased current density likely results from a hyperpolarized shift in open probability. These observations were supported by computational neuron modeling in which four of the five variants we examined, in which voltage dependence of activation was either hyperpolarized or unchanged, promoted overt hyperexcitability in an immature neuron where Na$_V$1.2N is the sole sodium channel in the AIS and the nodes of Ranvier. Furthermore, recent work has suggested that shifts in voltage dependence of activation more strongly influence neuronal excitability than shifts in voltage dependence of inactivation (Liu et al., 2019). Work by Hu and Bean (2018) showed that a 3-mV shift in voltage dependence of channel activation may lead to up to twice as many sodium channels being recruited due to the steep slope of voltage-dependent channel activation. Thus, even small shifts in voltage dependence of activation may lead to greater recruitment of sodium channels in response to subthreshold events. Consistent with this, T1623N and R1882Q, which show depolarized voltage dependence of inactivation, show only modestly increased excitability.

One variant in our study, R1882Q, has been studied previously by two groups (Berecki et al., 2018; Mason et al., 2019). Our primary finding for this variant was a depolarized shift in voltage dependence of inactivation, as well as slower onset of inactivation. The previous studies showed similar effects on these parameters. However, Berecki et al. (2018) also observed larger whole-cell sodium current compared with the WT

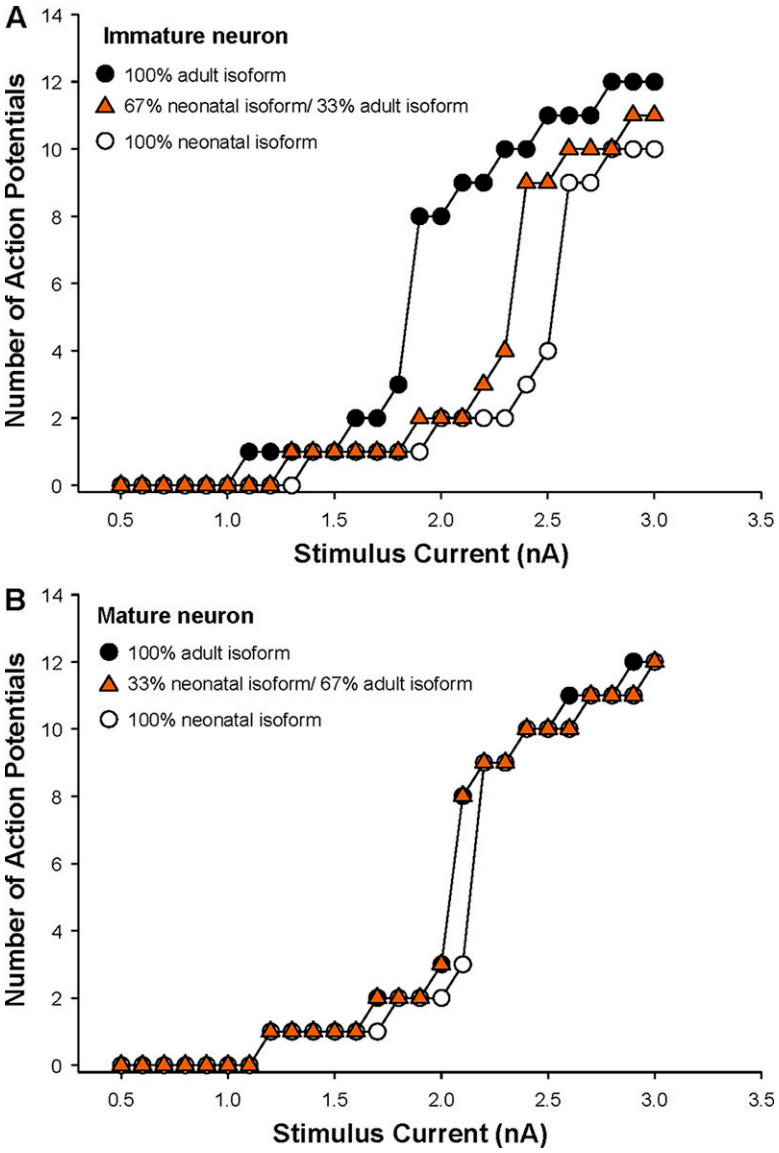

Figure 9. **Alternative splicing of $Na_V1.2$ modulates neuronal excitability. (A)** Summary data plotting the number of action potentials against stimulation current for an immature neuron with specific ratios of neonatal/adult $Na_V1.2$ isoforms. **(B)** Summary data plotting the number of action potentials against stimulation current for a mature neuron with specific ratios of neonatal/adult $Na_V1.2$ isoforms.

channel. Neither our results nor the results of Mason et al. (2019) showed larger currents mediated by the R1882Q mutation. Considering that Berecki et al. (2018) performed experiments in Chinese hamster ovary cells, while our work and the study by Mason et al. (2019) used human embryonic kidney–derived cell lines, the most likely explanation for discrepancies between these studies is different cell types.

Other human $Na_V1.2$ variants are associated with BFNIS, which exhibits an early onset of pharmacoresponsive epilepsy that typically remits within the first year of life (Xu et al., 2007; Misra et al., 2008). Functional evaluation of BFNIS-associated variants have mostly demonstrated subtle alterations of channel properties, such as small hyperpolarized shifts in voltage dependence of activation or enhanced persistent current, which are consistent with mild gain of function. Two specific *SCN2A* variants, M252V and L1563V, exhibit biophysical defects only when studied in $Na_V1.2N$ (Xu et al., 2007; Liao et al., 2010). By contrast, one variant (V261M) exhibited functional abnormalities only when expressed in $Na_V1.2A$ (Liao et al., 2010). These findings were interpreted as evidence against the hypothesis that remission of epilepsy in BFNIS occurs following the developmental switch in *SCN2A* alternative splicing, but that remission is due to higher expression of $Na_V1.6$ in these cells, which limits the functional contribution of $Na_V1.2$. Consistent with this notion, computational simulations of $Na_V1.2$-L1563V demonstrated only modestly increased excitability in immature neurons that normalized in the mature neuron (Xu et al., 2007).

Different functional consequences of mutant $Na_V1.2$ channels due to alternative splicing is unlikely to be the only factor accounting for early-onset epilepsy and the subsequent severe neurodevelopmental impairments seen in epileptic encephalopathies. Early neuronal injury and subsequent tissue responses (e.g., reactive gliosis, inflammation) likely contribute to the perpetuation of the seizure-prone state (Loewen et al., 2016). A greater proclivity to seizure initiation during early development may be the primary contributing factor of enhanced channel dysfunction of mutant $Na_V1.2N$. Indeed, our computational models with reduced potassium conductance show that

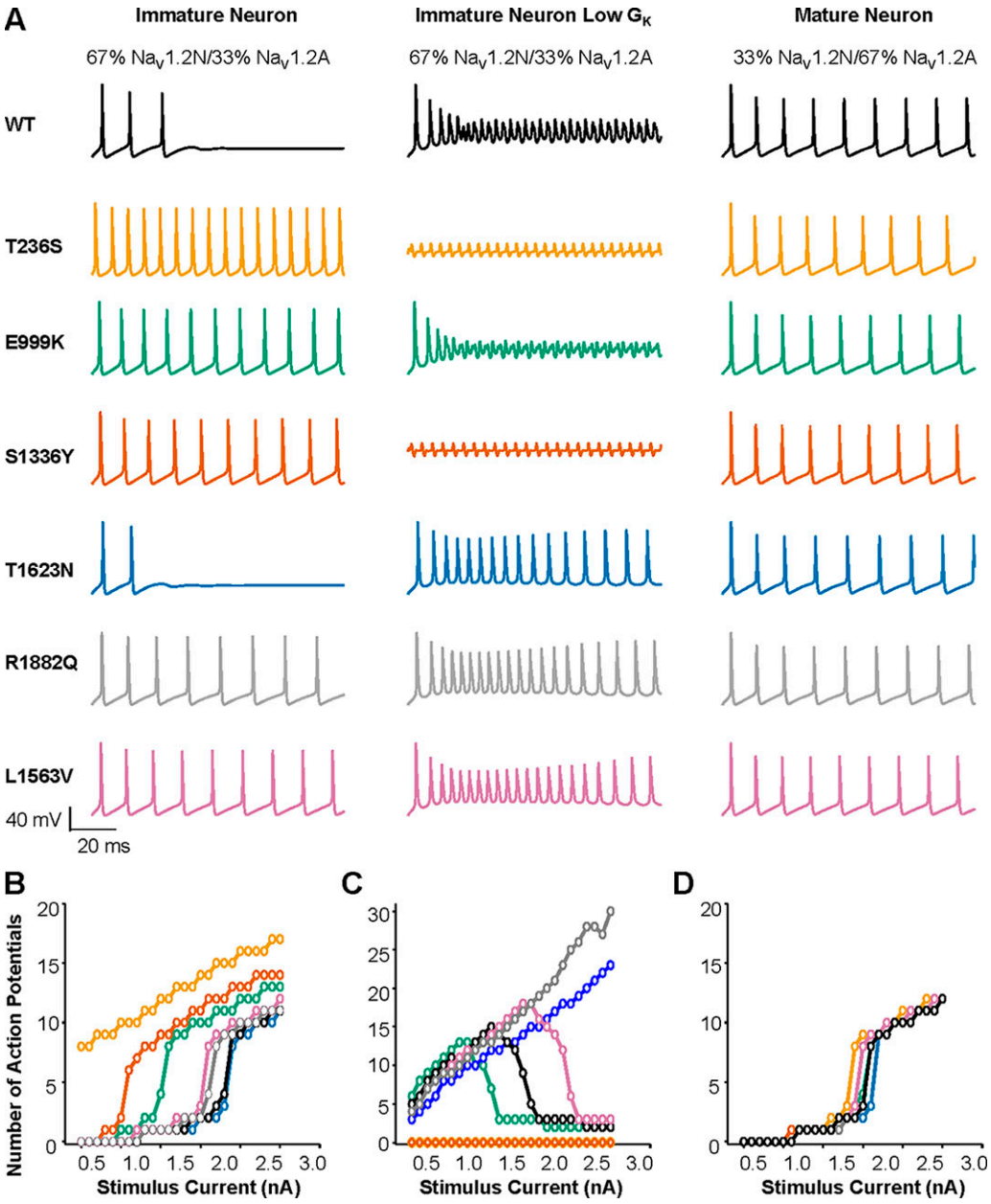

Figure 10. **Neuronal maturity influences hyperexcitability associated with Na$_V$1.2 variants. (A)** Action potentials generated in response to a 2.2-nA somatic current stimulation for an immature neuron expressing 67% Na$_V$1.2N and 33% Na$_V$1.2A throughout the AIS (left), an immature neuron expressing 67% Na$_V$1.2N and 33% Na$_V$1.2A throughout the AIS, and lower potassium conductance (middle), and a mature neuron expressing 33% Na$_V$1.2N and 67% Na$_V$1.2A restricted to the proximal AIS (right). **(B)** Summary data plotting the number of action potentials against stimulation current for the immature neuron defined in A. **(C)** Summary data plotting the number of action potentials against stimulation current for the immature neuron with low potassium conductance defined in A. **(D)** Summary data plotting the number of action potentials against stimulation current for the mature neuron defined in A. All simulations assumed heterozygosity.

EOEE-associated variants are prone to hyperexcitability very early in development, likely causing lasting changes to network development.

Many functional and genetic changes occur during the course of neuronal development. As stated above, there is a developmentally regulated switch between the neonatal and adult isoforms of Na$_V$1.2 and escalating potassium conductance. However, it is apparent from previous studies that the switch is not complete, with some neonatal isoform persisting into adulthood (Gazina et al., 2010). Further, during the course of neuronal development, Na$_V$1.2 is replaced in the distal AIS and the nodes of Ranvier by Na$_V$1.6 (Liao et al., 2010). Our neuron simulations demonstrated that when EOEE-associated variants are present in both Na$_V$1.2N and Na$_V$1.2A in a developing neuron, the presence of the less severely affected adult isoform dampens the effect of the neonatal isoform, rendering the neuron less excitable than when the neonatal isoform is the sole Na$_V$ channel. Interestingly, when these mutant channels are

incorporated into an adult neuron model where $Na_V1.6$ is largely responsible for action potential initiation and propagation, we see that no variant dramatically affects excitability. These results suggest that EOEE-associated $Na_V1.2$ variants (T236S, E999K, S1336Y, T1623N, and R1882Q) exert their effects very early in development, as is typical for other epileptic encephalopathies such as Dravet syndrome. While replacement of $Na_V1.2$ at the AIS by $Na_V1.6$ later in development may modulate seizures later in life, it is reasonable to predict that maladaptive changes in neuronal physiology occur in response to dysfunction of $Na_V1.2$ early in development.

An important consideration of our work is that we are examining the effect of channel variants in a model of a cortical pyramidal neuron, due to the high expression of $Na_V1.2$ throughout the neocortex during development and persistent expression throughout adulthood (Spratt et al., 2019). However, there is some evidence that $Na_V1.2$ is expressed at the AIS of some interneurons, where it either mediates spontaneous action potential firing associated with basal network inhibition or is critical for network disinhibition (Ye et al., 2018). Ye et al. (2018) showed that epileptiform activity induced by magnesium deprivation was exacerbated by selective inhibition of $Na_V1.2$ with low concentrations of phrixotoxin-3 in cortical slices. This abnormal activity could be normalized by inhibition of GABA-mediated neurotransmission (Ye et al., 2018). Additionally, $Na_V1.2$ is found in unmyelinated axons of neurons from the hippocampal dentate, cerebellar granule cells, and medium spiny neurons of the striatum (Westenbroek et al., 1989; Gong et al., 1999; Miyazaki et al., 2014). Simulations of neuronal excitability suggested that the adult isoforms of two variants we studied, S1336Y and T1623N, are associated with lower neuronal excitability where $Na_V1.2$ is the only channel at the AIS, while the neonatal isoform showed either dramatic (S1336Y) or modest (T1623N) hyperexcitability. Because these mutant channels do not influence neuronal excitability in an adult cortical pyramidal neuron, it is possible that complex network effects are set in place by having hyperexcitability during network development. Alternatively, loss of function of small populations of inhibitory interneurons may significantly disrupt excitation/inhibition balance.

In summary, our work has demonstrated that *SCN2A*-associated EOEE may result from channel gain of function that is potentiated in the neonatal $Na_V1.2N$ proteoform. Further, the developmental stage of the neuron, including $Na_V1.2$ splice proteoform ratio, total Na_V channel composition, and total potassium conductance, are critical determinants of neuronal excitability and are important considerations for functional evaluation of $Na_V1.2$ variants associated with early-onset epilepsy.

Acknowledgments

Merritt C. Maduke served as editor.

We thank Jennifer D. Kunic for technical assistance with the project.

This work was funded in part by grants from the National Institutes of Health (U54-NS108874), grants from the Simons Foundation Autism Research Initiative to A.L. George Jr. and K.J. Bender (513133 to K.J. Bender), and a generous gift from the Davee Foundation.

The authors declare no competing financial interests.

Author contributions: C.H. Thompson, R. Ben-Shalom, K.J. Bender, and A.L. George Jr. designed the research; C.H. Thompson and R. Ben-Shalom performed experiments; C.H. Thompson and R. Ben-Shalom analyzed data; and C.H. Thompson, R. Ben-Shalom, K.J. Bender, and A.L. George Jr. wrote the paper.

Submitted: 11 July 2019
Accepted: 7 January 2020

References

Baasch, A.L., I. Hüning, C. Gilissen, J. Klepper, J.A. Veltman, G. Gillessen-Kaesbach, A. Hoischen, and K. Lohmann. 2014. Exome sequencing identifies a de novo SCN2A mutation in a patient with intractable seizures, severe intellectual disability, optic atrophy, muscular hypotonia, and brain abnormalities. *Epilepsia.* 55:e25–e29. https://doi.org/10.1111/epi.12554

Beal, J.C., K. Cherian, and S.L. Moshe. 2012. Early-onset epileptic encephalopathies: Ohtahara syndrome and early myoclonic encephalopathy. *Pediatr. Neurol.* 47:317–323. https://doi.org/10.1016/j.pediatrneurol.2012.06.002

Ben-Shalom, R., C.M. Keeshen, K.N. Berrios, J.Y. An, S.J. Sanders, and K.J. Bender. 2017. Opposing Effects on $Na_V1.2$ Function Underlie Differences Between SCN2A Variants Observed in Individuals With Autism Spectrum Disorder or Infantile Seizures. *Biol. Psychiatry.* 82:224–232. https://doi.org/10.1016/j.biopsych.2017.01.009

Berecki, G., K.B. Howell, Y.H. Deerasooriya, M.R. Cilio, M.K. Oliva, D. Kaplan, I.E. Scheffer, S.F. Berkovic, and S. Petrou. 2018. Dynamic action potential clamp predicts functional separation in mild familial and severe de novo forms of *SCN2A* epilepsy. *Proc. Natl. Acad. Sci. USA.* 115:E5516–E5525. https://doi.org/10.1073/pnas.1800077115

Berkovic, S.F., S.E. Heron, L. Giordano, C. Marini, R. Guerrini, R.E. Kaplan, A. Gambardella, O.K. Steinlein, B.E. Grinton, J.T. Dean, et al. 2004. Benign familial neonatal-infantile seizures: characterization of a new sodium channelopathy. *Ann. Neurol.* 55:550–557. https://doi.org/10.1002/ana.20029

Chen, C., V. Bharucha, Y. Chen, R.E. Westenbroek, A. Brown, J.D. Malhotra, D. Jones, C. Avery, P.J. Gillespie III, K.A. Kazen-Gillespie, et al. 2002. Reduced sodium channel density, altered voltage dependence of inactivation, and increased susceptibility to seizures in mice lacking sodium channel beta 2-subunits. *Proc. Natl. Acad. Sci. USA.* 99:17072–17077. https://doi.org/10.1073/pnas.212638099

Copley, R.R. 2004. Evolutionary convergence of alternative splicing in ion channels. *Trends Genet.* 20:171–176. https://doi.org/10.1016/j.tig.2004.02.001

D'Gama, A.M., S. Pochareddy, M. Li, S.S. Jamuar, R.E. Reiff, A.N. Lam, N. Sestan, and C.A. Walsh. 2015. Targeted DNA Sequencing from Autism Spectrum Disorder Brains Implicates Multiple Genetic Mechanisms. *Neuron.* 88:910–917. https://doi.org/10.1016/j.neuron.2015.11.009

Diss, J.K., S.P. Fraser, and M.B. Djamgoz. 2004. Voltage-gated Na+ channels: multiplicity of expression, plasticity, functional implications and pathophysiological aspects. *Eur. Biophys. J.* 33:180–193. https://doi.org/10.1007/s00249-004-0389-0

Estacion, M., J.E. O'Brien, A. Conravey, M.F. Hammer, S.G. Waxman, S.D. Dib-Hajj, and M.H. Meisler. 2014. A novel de novo mutation of SCN8A (Nav1.6) with enhanced channel activation in a child with epileptic encephalopathy. *Neurobiol. Dis.* 69:117–123. https://doi.org/10.1016/j.nbd.2014.05.017

Gazina, E.V., B.T. Leaw, K.L. Richards, V.C. Wimmer, T.H. Kim, T.D. Aumann, T.J. Featherby, L. Churilov, V.E. Hammond, C.A. Reid, and S. Petrou. 2015. 'Neonatal' Nav1.2 reduces neuronal excitability and affects seizure susceptibility and behaviour. *Hum. Mol. Genet.* 24:1457–1468. https://doi.org/10.1093/hmg/ddu562

Gazina, E.V., K.L. Richards, M.B. Mokhtar, E.A. Thomas, C.A. Reid, and S. Petrou. 2010. Differential expression of exon 5 splice variants of sodium

channel alpha subunit mRNAs in the developing mouse brain. *Neuroscience.* 166:195–200. https://doi.org/10.1016/j.neuroscience.2009.12.011

George, A.L. Jr. 2005. Inherited disorders of voltage-gated sodium channels. *J. Clin. Invest.* 115:1990–1999. https://doi.org/10.1172/JCI25505

Gong, B., K.J. Rhodes, Z. Bekele-Arcuri, and J.S. Trimmer. 1999. Type I and type II Na(+) channel alpha-subunit polypeptides exhibit distinct spatial and temporal patterning, and association with auxiliary subunits in rat brain. *J. Comp. Neurol.* 412:342–352. https://doi.org/10.1002/(SICI)1096-9861(19990920)412:2<342::AID-CNE11>3.0.CO;2-2

Guan, D., L.R. Horton, W.E. Armstrong, and R.C. Foehring. 2011. Postnatal development of A-type and Kv1- and Kv2-mediated potassium channel currents in neocortical pyramidal neurons. *J. Neurophysiol.* 105:2976–2988. https://doi.org/10.1152/jn.00758.2010

Hallermann, S., C.P. de Kock, G.J. Stuart, and M.H. Kole. 2012. State and location dependence of action potential metabolic cost in cortical pyramidal neurons. *Nat. Neurosci.* 15:1007–1014. https://doi.org/10.1038/nn.3132

Herlenius, E., S.E. Heron, B.E. Grinton, D. Keay, I.E. Scheffer, J.C. Mulley, and S.F. Berkovic. 2007. SCN2A mutations and benign familial neonatal-infantile seizures: the phenotypic spectrum. *Epilepsia.* 48:1138–1142. https://doi.org/10.1111/j.1528-1167.2007.01049.x

Heron, S.E., K.M. Crossland, E. Andermann, H.A. Phillips, A.J. Hall, A. Bleasel, M. Shevell, S. Mercho, M.H. Seni, M.C. Guiot, et al. 2002. Sodium-channel defects in benign familial neonatal-infantile seizures. *Lancet.* 360:851–852. https://doi.org/10.1016/S0140-6736(02)09968-3

Howell, K.B., J.M. McMahon, G.L. Carvill, D. Tambunan, M.T. Mackay, V. Rodriguez-Casero, R. Webster, D. Clark, J.L. Freeman, S. Calvert, et al. 2015. SCN2A encephalopathy: A major cause of epilepsy of infancy with migrating focal seizures. *Neurology.* 85:958–966. https://doi.org/10.1212/WNL.0000000000001926

Hu, W., and B.P. Bean. 2018. Differential Control of Axonal and Somatic Resting Potential by Voltage-Dependent Conductances in Cortical Layer 5 Pyramidal Neurons. *Neuron.* 99:1355. https://doi.org/10.1016/j.neuron.2018.08.042

Hu, W., C. Tian, T. Li, M. Yang, H. Hou, and Y. Shu. 2009. Distinct contributions of Na(v)1.6 and Na(v)1.2 in action potential initiation and backpropagation. *Nat. Neurosci.* 12:996–1002. https://doi.org/10.1038/nn.2359

Isom, L.L., K.S. De Jongh, D.E. Patton, B.F.X. Reber, J. Offord, H. Charbonneau, K. Walsh, A.L. Goldin, and W.A. Catterall. 1992. Primary structure and functional expression of the beta 1 subunit of the rat brain sodium channel. *Science.* 256:839–842. https://doi.org/10.1126/science.1375395

Isom, L.L., D.S. Ragsdale, K.S. De Jongh, R.E. Westenbroek, B.F.X. Reber, T. Scheuer, and W.A. Catterall. 1995. Structure and function of the beta 2 subunit of brain sodium channels, a transmembrane glycoprotein with a CAM motif. *Cell.* 83:433–442. https://doi.org/10.1016/0092-8674(95)90121-3

Kahlig, K.M., T.H. Rhodes, M. Pusch, T. Freilinger, J.M. Pereira-Monteiro, M.D. Ferrari, A.M. van den Maagdenberg, M. Dichgans, and A.L. George Jr. 2008. Divergent sodium channel defects in familial hemiplegic migraine. *Proc. Natl. Acad. Sci. USA.* 105:9799–9804. https://doi.org/10.1073/pnas.0711717105

Kasai, N., K. Fukushima, Y. Ueki, S. Prasad, J. Nosakowski, K. Sugata, A. Sugata, K. Nishizaki, N.C. Meyer, and R.J. Smith. 2001. Genomic structures of SCN2A and SCN3A - candidate genes for deafness at the DFNA16 locus. *Gene.* 264:113–122. https://doi.org/10.1016/S0378-1119(00)00594-1

Le Bouter, S., S. Demolombe, A. Chambellan, C. Bellocq, F. Aimond, G. Toumaniantz, G. Lande, S. Siavoshian, I. Baró, A.L. Pond, et al. 2003. Microarray analysis reveals complex remodeling of cardiac ion channel expression with altered thyroid status: relation to cellular and integrated electrophysiology. *Circ. Res.* 92:234–242. https://doi.org/10.1161/01.RES.0000053185.75505.8E

Liao, Y., L. Deprez, S. Maljevic, J. Pitsch, L. Claes, D. Hristova, A. Jordanova, S. Ala-Mello, A. Bellan-Koch, D. Blazevic, et al. 2010. Molecular correlates of age-dependent seizures in an inherited neonatal-infantile epilepsy. *Brain.* 133:1403–1414. https://doi.org/10.1093/brain/awq057

Liu, Y., J. Schubert, L. Sonnenberg, K.L. Helbig, C.E. Hoei-Hansen, M. Koko, M. Rannap, S. Lauxmann, M. Huq, M.C. Schneider, et al. 2019. Neuronal mechanisms of mutations in SCN8A causing epilepsy or intellectual disability. *Brain.* 142:376–390. https://doi.org/10.1093/brain/awy326

Loewen, J.L., M.L. Barker-Haliski, E.J. Dahle, H.S. White, and K.S. Wilcox. 2016. Neuronal Injury, Gliosis, and Glial Proliferation in Two Models of Temporal Lobe Epilepsy. *J. Neuropathol. Exp. Neurol.* 75:366–378. https://doi.org/10.1093/jnen/nlw008

Lopez-Santiago, L.F., Y. Yuan, J.L. Wagnon, J.M. Hull, C.R. Frasier, H.A. O'Malley, M.H. Meisler, and L.L. Isom. 2017. Neuronal hyperexcitability in a mouse model of *SCN8A* epileptic encephalopathy. *Proc. Natl. Acad. Sci. USA.* 114:2383–2388. https://doi.org/10.1073/pnas.1616821114

Lossin, C., D.W. Wang, T.H. Rhodes, C.G. Vanoye, and A.L. George Jr. 2002. Molecular basis of an inherited epilepsy. *Neuron.* 34:877–884. https://doi.org/10.1016/S0896-6273(02)00714-6

Mason, E.R., F. Wu, R.R. Patel, Y. Xiao, S.C. Cannon, and T.R. Cummins. 2019. Resurgent and Gating Pore Currents Induced by *De Novo SCN2A* Epilepsy Mutations. *eNeuro.* 6:ENEURO.0141-19.2019.

Misra, S.N., K.M. Kahlig, and A.L. George Jr. 2008. Impaired NaV1.2 function and reduced cell surface expression in benign familial neonatal-infantile seizures. *Epilepsia.* 49:1535–1545. https://doi.org/10.1111/j.1528-1167.2008.01619.x

Miyazaki, H., F. Oyama, R. Inoue, T. Aosaki, T. Abe, H. Kiyonari, Y. Kino, M. Kurosawa, J. Shimizu, I. Ogiwara, et al. 2014. Singular localization of sodium channel β4 subunit in unmyelinated fibres and its role in the striatum. *Nat. Commun.* 5:5525. https://doi.org/10.1038/ncomms6525

Nakamura, K., M. Kato, H. Osaka, S. Yamashita, E. Nakagawa, K. Haginoya, J. Tohyama, M. Okuda, T. Wada, S. Shimakawa, et al. 2013. Clinical spectrum of SCN2A mutations expanding to Ohtahara syndrome. *Neurology.* 81:992–998. https://doi.org/10.1212/WNL.0b013e3182a43e57

O'Roak, B.J., P. Deriziotis, C. Lee, L. Vives, J.J. Schwartz, S. Girirajan, E. Karakoc, A.P. Mackenzie, S.B. Ng, C. Baker, et al. 2011. Exome sequencing in sporadic autism spectrum disorders identifies severe de novo mutations. *Nat. Genet.* 43:585–589. https://doi.org/10.1038/ng.835

Ogiwara, I., K. Ito, Y. Sawaishi, H. Osaka, E. Mazaki, I. Inoue, M. Montal, T. Hashikawa, T. Shike, T. Fujiwara, et al. 2009. De novo mutations of voltage-gated sodium channel alphaII gene SCN2A in intractable epilepsies. *Neurology.* 73:1046–1053. https://doi.org/10.1212/WNL.0b013e3181b9cebc

Ogiwara, I., H. Miyamoto, N. Morita, N. Atapour, E. Mazaki, I. Inoue, T. Takeuchi, S. Itohara, Y. Yanagawa, K. Obata, et al. 2007. $Na_v1.1$ localizes to axons of parvalbumin-positive inhibitory interneurons: a circuit basis for epileptic seizures in mice carrying an *Scn1a* gene mutation. *J. Neurosci.* 27:5903–5914. https://doi.org/10.1523/JNEUROSCI.5270-06.2007

Oliva, M., S.F. Berkovic, and S. Petrou. 2012. Sodium channels and the neurobiology of epilepsy. *Epilepsia.* 53:1849–1859. https://doi.org/10.1111/j.1528-1167.2012.03631.x

Onkal, R., J.H. Mattis, S.P. Fraser, J.K. Diss, D. Shao, K. Okuse, and M.B. Djamgoz. 2008. Alternative splicing of Nav1.5: an electrophysiological comparison of 'neonatal' and 'adult' isoforms and critical involvement of a lysine residue. *J. Cell. Physiol.* 216:716–726. https://doi.org/10.1002/jcp.21451

Rhodes, T.H., C. Lossin, C.G. Vanoye, D.W. Wang, and A.L. George Jr. 2004. Noninactivating voltage-gated sodium channels in severe myoclonic epilepsy of infancy. *Proc. Natl. Acad. Sci. USA.* 101:11147–11152. https://doi.org/10.1073/pnas.0402482101

Sanders, S.J., A.J. Campbell, J.R. Cottrell, R.S. Moller, F.F. Wagner, A.L. Auldridge, R.A. Bernier, W.A. Catterall, W.K. Chung, J.R. Empfield, et al. 2018. Progress in Understanding and Treating SCN2A-Mediated Disorders. *Trends Neurosci.* 41:442–456. https://doi.org/10.1016/j.tins.2018.03.011

Sanders, S.J., M.T. Murtha, A.R. Gupta, J.D. Murdoch, M.J. Raubeson, A.J. Willsey, A.G. Ercan-Sencicek, N.M. DiLullo, N.N. Parikshak, J.L. Stein, et al. 2012. De novo mutations revealed by whole-exome sequencing are strongly associated with autism. *Nature.* 485:237–241. https://doi.org/10.1038/nature10945

Schmidt-Hieber, C., and J. Bischofberger. 2010. Fast sodium channel gating supports localized and efficient axonal action potential initiation. *J. Neurosci.* 30:10233–10242. https://doi.org/10.1523/JNEUROSCI.6335-09.2010

Spratt, P.W.E., R. Ben-Shalom, C.M. Keeshen, K.J. Burke Jr., R.L. Clarkson, S.J. Sanders, and K.J. Bender. 2019. The Autism-Associated Gene Scn2a Contributes to Dendritic Excitability and Synaptic Function in the Prefrontal Cortex. *Neuron.* 103:673–685.e5. https://doi.org/10.1016/j.neuron.2019.05.037

Thompson, C.H., K.M. Kahlig, and A.L. George Jr. 2011. SCN1A splice variants exhibit divergent sensitivity to commonly used antiepileptic drugs. *Epilepsia.* 52:1000–1009. https://doi.org/10.1111/j.1528-1167.2011.03040.x

Thompson, C.H., J.C. Porter, K.M. Kahlig, M.A. Daniels, and A.L. George Jr. 2012. Nontruncating SCN1A mutations associated with severe myoclonic epilepsy of infancy impair cell surface expression.

J. Biol. Chem. 287:42001–42008. https://doi.org/10.1074/jbc.M112.421883

Tian, C., K. Wang, W. Ke, H. Guo, and Y. Shu. 2014. Molecular identity of axonal sodium channels in human cortical pyramidal cells. *Front. Cell. Neurosci.* 8:297. https://doi.org/10.3389/fncel.2014.00297

Touma, M., M. Joshi, M.C. Connolly, P.E. Grant, A.R. Hansen, O. Khwaja, G.T. Berry, H.C. Kinney, A. Poduri, and P.B. Agrawal. 2013. Whole genome sequencing identifies SCN2A mutation in monozygotic twins with Ohtahara syndrome and unique neuropathologic findings. *Epilepsia*. 54: e81–e85. https://doi.org/10.1111/epi.12137

Uebachs, M., T. Opitz, M. Royeck, G. Dickhof, M.T. Horstmann, L.L. Isom, and H. Beck. 2010. Efficacy loss of the anticonvulsant carbamazepine in mice lacking sodium channel beta subunits via paradoxical effects on persistent sodium currents. *J. Neurosci.* 30:8489–8501. https://doi.org/10.1523/JNEUROSCI.1534-10.2010

Wagnon, J.L., B.S. Barker, J.A. Hounshell, C.A. Haaxma, A. Shealy, T. Moss, S. Parikh, R.D. Messer, M.K. Patel, and M.H. Meisler. 2015. Pathogenic mechanism of recurrent mutations of SCN8A in epileptic encephalopathy. *Ann. Clin. Transl. Neurol.* 3:114–123. https://doi.org/10.1002/acn3.276

Westenbroek, R.E., D.K. Merrick, and W.A. Catterall. 1989. Differential subcellular localization of the RI and RII Na+ channel subtypes in central neurons. *Neuron.* 3:695–704. https://doi.org/10.1016/0896-6273(89)90238-9

Wolff, M., K.M. Johannesen, U.B.S. Hedrich, S. Masnada, G. Rubboli, E. Gardella, G. Lesca, D. Ville, M. Milh, L. Villard, et al. 2017. Genetic and phenotypic heterogeneity suggest therapeutic implications in SCN2A-related disorders. *Brain.* 140:1316–1336. https://doi.org/10.1093/brain/awx054

Xu, R., E.A. Thomas, M. Jenkins, E.V. Gazina, C. Chiu, S.E. Heron, J.C. Mulley, I.E. Scheffer, S.F. Berkovic, and S. Petrou. 2007. A childhood epilepsy mutation reveals a role for developmentally regulated splicing of a sodium channel. *Mol. Cell. Neurosci.* 35:292–301. https://doi.org/10.1016/j.mcn.2007.03.003

Yamagata, T., I. Ogiwara, E. Mazaki, Y. Yanagawa, and K. Yamakawa. 2017. Nav1.2 is expressed in caudal ganglionic eminence-derived disinhibitory interneurons: Mutually exclusive distributions of Nav1.1 and Nav1.2. *Biochem. Biophys. Res. Commun.* 491:1070–1076. https://doi.org/10.1016/j.bbrc.2017.08.013

Ye, M., J. Yang, C. Tian, Q. Zhu, L. Yin, S. Jiang, M. Yang, and Y. Shu. 2018. Differential roles of $Na_V1.2$ and $Na_V1.6$ in regulating neuronal excitability at febrile temperature and distinct contributions to febrile seizures. *Sci. Rep.* 8:753. https://doi.org/10.1038/s41598-017-17344-8

Yu, F.H., M. Mantegazza, R.E. Westenbroek, C.A. Robbins, F. Kalume, K.A. Burton, W.J. Spain, G.S. McKnight, T. Scheuer, and W.A. Catterall. 2006. Reduced sodium current in GABAergic interneurons in a mouse model of severe myoclonic epilepsy in infancy. *Nat. Neurosci.* 9: 1142–1149. https://doi.org/10.1038/nn1754

Zerem, A., D. Lev, L. Blumkin, H. Goldberg-Stern, Y. Michaeli-Yossef, A. Halevy, S. Kivity, K. Nakamura, N. Matsumoto, E. Leshinsky-Silver, et al. 2014. Paternal germline mosaicism of a SCN2A mutation results in Ohtahara syndrome in half siblings. *Eur. J. Paediatr. Neurol.* 18:567–571. https://doi.org/10.1016/j.ejpn.2014.04.008